

A Non-Parametric Test of Variability of Type Ia Supernovae Luminosity and CDDR

**Darshan Kumar^a , Akshay Rana^b , Deepak Jain^c ,
Shobhit Mahajan^a , Amitabha Mukherjee^a , and R. F. L.
Holanda^{d,e,f}**

^aDepartment of Physics and Astrophysics, University of Delhi,
Delhi 110007, India

^bSt. Stephen's College, University of Delhi,
Delhi 110007, India

^cDeen Dayal Upadhyaya College, University of Delhi,
Dwarka, New Delhi 110078, India

^dDepartamento de Física, Universidade Federal do Rio Grande do Norte,
Natal-Rio Grande do Norte 59072-970, Brasil

^eBrasil Departamento de Física, Universidade Federal de Campina Grande,
Campina Grande - PB 58429-900, Brasil

^fDepartamento de Física, Universidade Federal de Sergipe,
Aracaju - SE 49100-000, Brazil

E-mail: dkumar1@physics.du.ac.in, akshay@ststephens.edu,
djain@ddu.du.ac.in, sm@physics.du.ac.in, am@physics.du.ac.in,
holandarfl@fisica.ufrn.br

Abstract. The first observational evidence for cosmic acceleration appeared from Type Ia supernovae (SNe Type Ia) Hubble diagram from two different groups. However, the empirical treatment of SNe Type Ia and their ability to show cosmic acceleration have been the subject of some debate in the literature. In this work we probe the assumption of redshift-independent absolute magnitude (M_B) of SNe along with its correlation with spatial curvature (Ω_{k0}) and cosmic distance duality relation (CDDR) parameter ($\eta(z)$). This work is divided into two parts. Firstly, we check the validity of CDDR which relates the luminosity distance (d_L) and angular diameter distance (d_A) via redshift. We use the Pantheon SNe Ia dataset combined with the $H(z)$ measurements derived from the cosmic chronometers. Further, four different redshift-dependent parametrizations of the distance duality parameter ($\eta(z)$) are used. The CDDR is fairly consistent for almost every parametrization within a 2σ confidence level in both flat and a non-flat universe. In the second part, we assume the validity of CDDR and emphasize on the variability of M_B and its correlation with Ω_{k0} . We choose four different redshift-dependent parametrizations of M_B . The results indicate no evolution of M_B within 2σ confidence level. For all parametrizations, the best fit value of Ω_{k0} indicates a flat universe at 2σ confidence level. However a mild inclination towards a non flat universe is also observed. We have also examined the dependence of the results on the choice of different priors for H_0 .

Keywords: supernova type Ia - standard candles, cosmological parameters from LSS, dark energy theory, cosmology of theories beyond the SM.

Contents

1	Introduction	1
2	Cosmological Probes and Data sets	4
2.1	Type Ia Supernovae measurement and Pantheon Sample	4
2.2	Constraining Angular Diameter Distance using $H(z)$ measurements	6
2.2.1	Hubble data set	6
2.2.2	Comoving distance using Gaussian Process	7
3	Analysis	9
4	Results	11
4.1	Test of CDDR	11
4.2	Test of variability of SNe Type Ia absolute luminosity	15
5	Discussion and Conclusions	20
	Bibliography	25

1 Introduction

The first observational evidence for the cosmic acceleration appeared from Type Ia supernovae (SNe Type Ia) observations performed by two different research groups [1, 2]. Over the decades, the number of SNe Type Ia catalogs have increased significantly. Even now, SNe Type Ia observations provide the most direct evidence for the current cosmic acceleration. In the context of Einstein’s General Theory of Relativity (GTR), SNe Type Ia observations support the existence of a mysterious form of energy called dark energy, that is either constant (Λ CDM) or slowly varying with time and space. (See reviews in Refs. [3–5]).

Type Ia supernovae (SNe Type Ia) are extremely luminous explosions and these are observationally identified by the absence of hydrogen and presence of silicon (Si II) spectral lines in their spectra [6]. The use of SNe Type Ia as a reliable cosmological probe relies on two fundamental assumptions:

a) The first assumption is that the shape of the light curve of all type Ia supernovae (SNe Type Ia) is similar; hence these can be standardized [7, 8]. In practice, this task of standardizing light curve of SNe Type Ia is achieved by using several empirically derived light curve fitters like, for instance, MLCS/MLCS2k2 [9], SALT [10], SALT2 [10], SiFTO [11] etc. As stated, the generalized functional forms of the light curves obtained in these fitters are purely empirical and based on plausible physical explanations to explain the light curves of SNe Type Ia from the time of explosion to a few weeks after peak brightness[12].

b) The second basic assumption behind the SNe Type Ia analysis is that the intrinsic luminosity of a supernova is independent of the redshift and the host galaxy environment. In other words, it is theoretically assumed that two different SNe Type Ia in two different host galaxies have the same intrinsic luminosity, independent of masses and redshifts of the host galaxies. However, in recent years several dedicated studies have concluded that the light curve fitting analysis of SNe Type Ia depends on their host galaxy masses [13]. Further, it is seen that SNe Type Ia events occurring in massive early-type, passive galaxies are brighter than those in late-type star forming galaxies [14–17].

The two main progenitor models of SNe Type Ia are the “single degenerate” and the “double degenerate” models. In the single degenerate model, a white dwarf accreting from a binary companion star is pushed over the Chandrasekhar mass limit, while in the double degenerate model of SNe Type Ia explosions, an orbiting pair of binary white dwarfs merge together and their mass eventually exceeds the Chandrasekhar mass limit. There is no established formalism to exactly differentiate between these two channels of SNe Type Ia explosion. Hence the observed supernova population catalog may have SNe Type Ia contributions coming from both these channels which will have a direct impact on the first and second assumptions used in SNe Type Ia analysis [18].

Further, the statistical treatment of SNe Type Ia, their dimming and their ability to prove the cosmic acceleration is still a topic of debate in the literature. This is because the process of obtaining the SNe Type Ia observations is not trivial but requires some priors for interpretations and corrections to convert an observed-frame magnitude to a rest-frame magnitude. Examples discussed in the literature are for instance: possible evolutionary effects in SNe Type Ia events [19, 20], local Hubble bubble [21, 22], modified gravity [23–25], unclustetered sources of light attenuation [26–29] and the existence of Axion-Like-Particles (ALPs) arising in a wide range of well-motivated high-energy physics scenarios. All these could also lead to the dimming of SNe Type Ia brightness [30, 31] which would eventually affect the second assumption used in the SNe Type Ia analysis.

Given the above mentioned limitations, Tutusaus et al. (2019) [32] relaxed the standard assumption that SNe Type Ia intrinsic luminosity is independent of the redshift and examined its impact on the cosmic acceleration. The authors reconstructed the expansion rate of the Universe by fitting the SNe Type Ia observations with a cubic spline interpolation. They showed that a non-accelerated expansion rate of the Universe is able to fit all the main background cosmological probes. In addition, Tutusaus et al. (2017) [33] found that when SNe Type Ia intrinsic luminosity is not assumed to be redshift independent, a non-accelerated low-redshift power law model is able to fit the low-redshift background data as well as the Λ CDM model. It has also been found that a significant correlation exists between SNe Type Ia luminosity (after the standardization) and the stellar population age at a 99.5% confidence level [34] indicating that the light-curve fitters used by the SNe Type Ia

community are not quite capable of correcting for the population age effect. More recently, Valentino et al. (2020) [35] have also raised the issue whether intrinsic SNe Type Ia luminosities might evolve with redshift. They analyse the impact of the latter on the inferred properties of the dark energy component responsible for cosmic acceleration. However, they find the evidence for cosmic acceleration to be robust to possible systematics. Along the same lines, Sapone et al. (2020) [36] also analyse the cosmological implications of an absolute luminosity of SNe Type Ia which could vary with respect to the redshift. Further, they study the impact of the latter on modified gravity models and non-homogeneous models.

These statements seem to offer enough plausible reasons to investigate the effects of variability of absolute luminosity of SNe Type Ia. However, these are not the sole reasons of concern about the variability of M_B . The cosmic acceleration rate and the cosmological parameters determined by the SNe Type Ia measurements are highly dependent on the possible dimming effect as well. Vavrycuk et al. (2019) [37] revived a debate about an origin of Type Ia supernova (SN Ia) dimming and showed that the standard Λ CDM model and the opaque universe model (caused by light extinction by intergalactic dust) fit the SN Ia measurements at redshifts $z < 1.4$ fairly well. Then, there are still some possible loopholes in the current SNe Type Ia observations and alternative mechanisms contributing to the acceleration evidence or even mimicking the dark energy behaviour have been proposed. It is important to point out that a constant value of the absolute luminosity of SNe Type Ia at the peak of its light curve is not sensitive to Hubble constant (H_0). Nevertheless, a variable absolute magnitude will be sensitive to H_0 .

These recent development motivate us to carry out a model independent study of finding any correlation between variable luminosity of SNe Type Ia and observed SNe Type Ia dimming effect due to opacity of the environment. The most general methodology of testing the cosmic opacity of SNe Type Ia is based on the cosmic distance duality relation (CDDR) which connects the luminosity distance d_L and angular diameter distance (ADD) d_A at the same redshift and is defined as, $d_L(1+z)^{-2}/d_A = \eta(z) = 1$. In order to look for the presence of some unknown physics phenomenon beyond the standard model or an inconsistency between cosmological data we check if $\eta(z) \neq 1$, that is CDDR is violated. This relation holds for general metric theories of gravity in any background, in which photons travel along null geodesics and the number of photons is conserved during cosmic evolution [38]. Briefly, the SNe Type Ia observations have been confronted with several other cosmological probes (strong gravitation lens systems, angular diameter distances, gas mass fractions, baryon acoustic oscillations, cosmic microwave background, radio sources, gravitational waves, $H(z)$ measurements, gamma ray bursts etc.) in order to put limits on the redshift dependence of η , that is on $\eta(z)$ [39–65]. All these works conclude that CDDR is valid within a 2σ confidence level. However, it is worth stressing that current analysis could not distinguish which functional form of $\eta(z)$ best describes the data (see details in Ref.[66]).

Another cosmological parameter which can be crucial to the variability of absolute luminosity of SNe Type Ia and its dimming effect is the cosmic curvature. Cosmic curvature (Ω_{k0}) is a fundamental geometric quantity of the Universe. It plays a crucial role in the evolution and dynamics of the universe. As, Ω_{k0} is directly related to cosmological distances, a flat or non-flat space-time would obviously impact the path travelled by the photon and eventually the absolute magnitude of SNe Type Ia. Hence, in this paper, we also probe the variation of the absolute luminosity of SNe Type Ia and its correlation with the CDDR parameter ($\eta(z)$) and cosmic curvature (Ω_{k0}).

For clarity of exposition, this paper is divided into two parts. In the first part, we test the validity of CDDR. We propose a new cosmological non-parametric test for CDDR by using SNe Type Ia observations and $H(z)$ measurements from cosmic chronometers. The basic procedure is as follows: we obtain the angular diameter distances at SNe Type Ia redshifts by applying Gaussian Process integration method on cosmic chronometer $H(z)$ data. By using a deformed CDDR of the form $d_L = \eta(z)d_A(1+z)^2$ and considering a flat universe, we impose limits on the SNe Type Ia absolute magnitude (M_B), and $\eta(z)$ functions, namely: $\eta(z) = \eta_0$, $\eta(z) = \eta_0 + \eta_1 z$, $\eta(z) = \eta_0 + \eta_1 z/(1+z)$ and $\eta(z) = \eta_0 + \eta_1 \ln(1+z)$.

After testing the validity of the CDDR parameter η in the first part, in the second part, we assume the validity of CDDR and put limits on the possible evolution of SNe Type Ia absolute magnitude by assuming $M_B(z) = M_{B0}$, $M_B(z) = M_{B0} + M_{B1}z$, $M_B(z) = M_{B0} + M_{B1}z/(1+z)$ and $M_B(z) = M_{B0} + M_{B1}\ln(1+z)$ parametrizations in flat and non flat cosmologies.

The structure of the paper is as follows: In Section 2, we discuss the cosmological probes and the data sets used in the analysis along with their theoretical construction. In Section 3, we outline the methodology used. In Section 4, the emphasis is on the results of both parts where in the first part we test the validity of CDDR and in the second part we test the variability of absolute luminosity of SNe Type Ia. Finally, in Section 5, we discuss the final outcomes of both parts and also explore the impact of different H_0 priors on our analysis.

2 Cosmological Probes and Data sets

In this section we present the cosmological probes and data sets used in the analysis.

2.1 Type Ia Supernovae measurement and Pantheon Sample

Type Ia supernovae are considered to be standard candles. Observations of these are at the core of establishing the validity of cosmic acceleration. The standard observable quantity in SNe Type Ia analysis is the distance modulus which is the

difference between the apparent and absolute magnitude of the SNe Type Ia. The observational measurement of this quantity is given by the relation

$$\mu_{\text{SN}} = m_{\text{B}}^{\text{obs}}(z) + \alpha \cdot X_1 - \beta \cdot \mathcal{C} - M_{\text{B}}. \quad (2.1)$$

where, m_{B} is the rest frame B-band observed peak magnitude, X_1 and \mathcal{C} are time stretching of the light curve and SNe Type Ia color at maximum brightness respectively and M_{B} is the absolute B-band magnitude. This relation indicates that the variability of the distance modulus is governed by two additional parameters X_1 and \mathcal{C} . It must be noted here that we do have two nuisance parameters α and β as well. In this paper we use the recent and largest database of SNe Type Ia known as the Pantheon data set. In this data set, these two nuisance parameters have been marginalized and eventually calibrated to be zero. This data set has 1048 SNe Type Ia measurements in the redshift range $0.01 \leq z \leq 2.26$ [13]. Hence, for the Pantheon data set, the observed distance modulus relaxes to the form $\mu_{\text{SN}} = m_{\text{B}}^{\text{obs}} - M_{\text{B}}$. Once we know the distance modulus, we can easily define the luminosity distance and uncertainty in observed luminosity distance as

$$d_{\text{L}}^{\text{th}}(z; M_{\text{B}}) = 10^{(m_{\text{B}}^{\text{th}} - M_{\text{B}} - 25)/5} (\text{Mpc}), \quad (2.2)$$

From Eq.(2.2), it can be easily seen that once we estimate the value of M_{B} , we can find the luminosity distance at a given redshift. However, in this work, our aim is to study the variation of the absolute magnitude (M_{B}) of SNe Type Ia, so if we can get a model-independent estimate of the luminosity distance from other observational probes then we can constrain the variability of M_{B} .

We use the cosmic distance duality relation (CDDR) to reconstruct the luminosity distance theoretically which is given by

$$d_{\text{L}}^{\text{th}}(z; \eta, \Omega_{k0}) = \eta(z) d_{\text{A}}(z; \Omega_{k0}) (1+z)^2. \quad (2.3)$$

Using Eq. (2.3) we can define, from Eq. (2.2), m_{B}^{th} as

$$m_{\text{B}}^{\text{th}}(z; \eta, M_{\text{B}}, \Omega_{k0}) = 5 \log \left(\eta(z) d_{\text{A}}(z; \Omega_{k0}) (1+z)^2 \right) + M_{\text{B}} + 25, \quad (2.4)$$

Here, η is the cosmic distance duality parameter which is a measure of the deviation from CDDR. CDDR holds for $\eta(z) = 1$. Here d_{L}^{th} is the theoretical luminosity distance defined in the terms of angular diameter distance d_{A} and $\eta(z)$. The angular diameter distance is defined as

$$d_{\text{A}}(z; H_0, \Omega_{k0}) = \begin{cases} \frac{d_H}{(1+z)\sqrt{\Omega_{k0}}} \sinh \left[\sqrt{\Omega_{k0}} \frac{d_C}{d_H} \right] & \text{for } \Omega_{k0} > 0. \\ \frac{d_C}{(1+z)} & \text{for } \Omega_{k0} = 0. \\ \frac{d_H}{(1+z)\sqrt{|\Omega_{k0}|}} \sin \left[\sqrt{|\Omega_{k0}|} \frac{d_C}{d_H} \right] & \text{for } \Omega_{k0} < 0. \end{cases} \quad (2.5)$$

Here Ω_{k0} is the cosmic curvature, where Ω_{k0} is greater, equal and less than zero for open, flat and closed universe respectively. d_C is the comoving distance and $d_H = c/H_0$ is known as the Hubble distance where c is the speed of light and H_0 is the Hubble constant.

2.2 Constraining Angular Diameter Distance using $H(z)$ measurements

As is evident from Eq. 2.5, if we can obtain a model-independent estimate of d_C/d_H then we can easily estimate angular diameter distance $d_A(z; \Omega_{k0})$ as a function of Ω_{k0} and subsequently theoretical luminosity distance $d_L^{\text{th}}(z; \eta, \Omega_{k0})$ as a function of η and Ω_{k0} . In this section we will first discuss the data sets and the methodology to obtain angular diameter distances from them.

2.2.1 Hubble data set

In cosmology, the Hubble parameter $H(z)$ is a crucial measured quantity which describes the dynamical properties of the universe such as the expansion rate and evolution history of the universe. It is also helpful to explore the nature of the dark energy. The most recent data compilation of Hubble parameter measurements [67] has 31 measurements of $H(z)$ which are obtained by using the differential ages of passively evolving galaxies. We now outline the steps needed to obtain the angular diameter distance that we need.

- (i) **Differential ages of passively evolving galaxies:** The Hubble parameter $H(z)$ can be expressed in the terms of the rate of change of cosmic time with the redshift, given by

$$H(z) = -\frac{1}{(1+z)} \frac{\Delta z}{\Delta t}. \quad (2.6)$$

The change of cosmic time with redshift can be estimated from the ageing of the stellar population in the galaxies. However, one needs to be extremely careful in selecting the galaxies while calculating the $H(z)$ values using this method. In young evolving galaxies, the stars are being born continuously and the emission spectra will be dominated by the young stellar population. Hence to estimate accurately the differential ageing of the universe, passively evolving red galaxies are used as their light is mostly dominated by the old stellar population [68]. To find $H(z)$ at a given redshift, the ages of the early type passively evolving galaxies with similar metallicity and very small redshift interval is calculated. The redshift difference Δz between two galaxies can be measured by using spectroscopic observations. For the estimation of Δt , [69] suggested the use of a direct spectroscopic observable (the 4000 Å break) which is known to be linearly related to the age of the stellar population of a galaxy at fixed metallicity. As the measure of $H(z)$ is estimated purely by

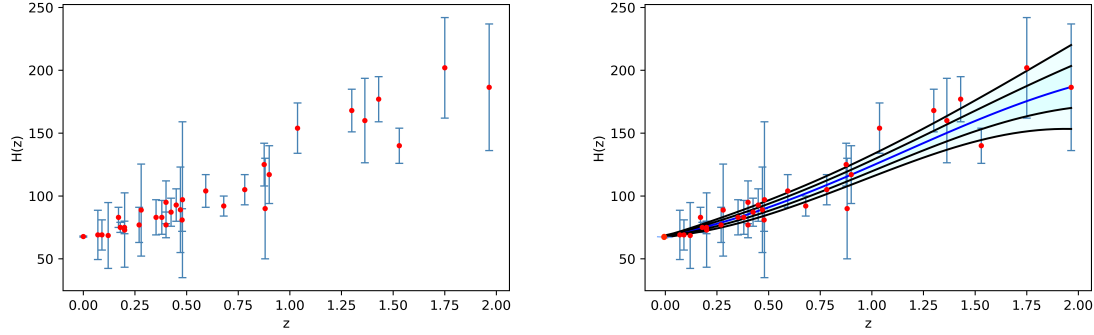


Figure 1: In the left plot, 31 CC $H(z)$ vs z datapoints are shown. In the right plot, $H(z)$ is estimated at all intermediate redshifts in the range $0 < z < 2$ using a non-parametric smoothing technique, namely Gaussian Process. In the analysis, the Hubble constant value is taken to be $H_0 = 67.66 \pm 0.42 \text{ km s}^{-1} \text{Mpc}^{-1}$ estimated from CMB measurement [75]. The impact of other choices of H_0 values on analysis has been discussed in Section 5(C).

using spectroscopic observations, it is independent of the cosmological model and has proved to be a strong probe to constrain cosmological models and assumptions. This method of calculating $H(z)$ is usually known as the “Cosmic Chronometers” and data points are generally referred to as CC $H(z)$. We have 31 data points estimated using this differential ages of passively evolving galaxies technique [69–74].

2.2.2 Comoving distance using Gaussian Process

In this analysis, we require a model-independent estimate of the angular diameter distance. For this, we first calculate the comoving distance d_C using the $H(z)$ measurement of cosmic chronometers as

$$\frac{d_C}{d_H} = \int_0^z \frac{dz'}{E(z')}. \quad (2.7)$$

Here $E(z) = H(z)/H_0$. If we have the functional form of $E(z)$ then we can easily integrate Eq. 2.7 by using any numerical integration method. However, in our case we have only $H(z)$ estimates at certain redshifts. In our analysis, to obtain continuous smooth values of $H(z)$ we use the Gaussian Process (GP), a well known hyper-parametric regression method [76]. GP has been widely used in the literature to reconstruct the shapes of physical functions and is very useful for such functional reconstructions due to its flexibility and simplicity. In this method, the complicated parametric relationship is replaced by parametrizing a probability model over the data. In mathematical terms, it is a distribution over functions, characterized by a mean function and covariance function, given by

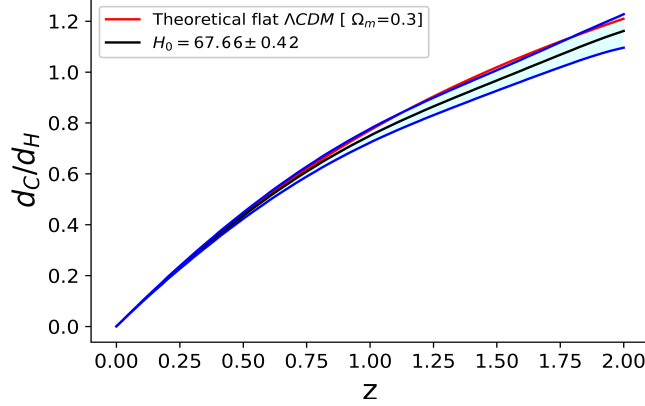


Figure 2: This plot represents the reconstructed values of d_C/d_H in the redshift in the range $0 < z < 2$. The solid black line represents the best fit line while blue lines includes the 1σ confidence region. The solid red line is the theoretical curve for the flat Λ CDM model with $\Omega_m = 0.3$. The value of H_0 used in reconstructing this plot is $H_0 = 67.66 \pm 0.42 \text{ km s}^{-1}\text{Mpc}^{-1}$.

$$K(z, z') = \langle (H(z) - \mu(z)) (H(z') - \mu(z')) \rangle \quad (2.8)$$

where $\mu(z)$ is the prior mean. In order to avoid model dependence appearing through the choice of the prior mean function, we have chosen it to be zero. This is a common choice of mean function as one can always normalize the data so it has zero mean. We have also checked by taking different values of prior mean, $\mu(z)$ and observed that the result is independent of the choice of the prior mean function. This method, however, comes with a few inherent underlying assumptions- it is assumed that each observation is an outcome of an independent Gaussian distribution belonging to the same population and the outcomes of observations at any two redshifts are correlated with the strength of correlation depending on their nearness to each other. We reconstructed our data by using the square exponential kernel function, given by

$$K(z, z') = \sigma_f^2 \exp\left(-\frac{(|z - z'|)^2}{2\ell^2}\right) \quad (2.9)$$

Here, σ_f and ℓ are two hyperparameters which control the amplitude and length-scale of the prior covariance. The value of hyperparameters is calculated by maximizing the corresponding marginal log-likelihood probability function of the distribution. For maximization, we use flat priors for σ_f and ℓ for all the choices of kernel function. In order to check the sensitivity of our analysis to the choice of the kernel function, we repeated our analysis with the Matérn-(3/2, 5/2, 7/2 & 9/2) kernel functions. Though the values of hyperparameters vary according to the choice of kernel function, the reconstructed curves do not show any significant deviation

from the curve obtained from square exponential curve. Hence we choose to work with the square exponential kernel function only.

Once we obtain the reconstructed $H(z)$ at all possible redshifts in the range $0 < z < 2$ as shown in Figure 1, we divide it by $H_0 = 67.66 \pm 0.42 \text{ km s}^{-1} \text{ Mpc}^{-1}$ value to obtain $E(z)$. We use the Simpson 3/8 method for numerically integrating Eq. 2.7 and obtain continuous values of d_C/d_H at all redshifts in the range $0 < z < 2$ which is shown in Figure 2. Further, we can use Eq. 2.5 to obtain the angular diameter distance as a function of cosmic curvature Ω_{k0} . The uncertainty in d_A i.e σ_{d_A} is estimated by propagating the error obtained in d_C/d_H using Gaussian Process.

3 Analysis

Generally, the Pantheon dataset comes in terms of SNe Type Ia apparent magnitudes and with a full covariance matrix¹, C_{sys} correlating the apparent magnitudes at various redshifts. This covariance matrix is a non-diagonal matrix of systematic uncertainties that come from the bias corrections method[13, 77].

In this analysis, we have to fit simultaneously three parameters i.e. M_B , η and Ω_{k0} . These parameters are determined by maximizing the likelihood $\mathcal{L} \sim \exp(-\chi^2/2)$, where chi-square (χ^2) is a quantity summed over all the Pantheon SNe Type Ia Sample redshifts, and is defined as

$$\chi_{\text{Pan}}^2 = \Delta m^T \cdot C^{-1} \cdot \Delta m \quad (3.1)$$

where, $C = D_{\text{stat}} + C_{\text{sys}}$. Here D_{stat} is the diagonal covariance matrix of the statistical uncertainties and $\Delta m = m_B^{\text{obs}}(z_i) - m_B^{\text{th}}(z_i; \eta, M_B, \Omega_{k0})$ which is given in Eqs.(2.1,2.4).

In this analysis, we have three unknown parameters, namely, the absolute magnitude of SNe Type Ia, M_B , the cosmic distance duality parameter, $\eta(z)$, and the cosmic curvature, Ω_{k0} . In order to investigate the variability of M_B we have to analyse its correlation with the remaining two parameters. In order to do so, we divide the work into two parts:

Part I: Test of CDDR

In this part, we consider the distance duality relation parameter (η) to test CDDR and put constraints on $\eta(z)$ simultaneously with the other two parameters i.e. M_B and Ω_{k0} . We take into account four parametrizations of $\eta(z)$ which are as follows

- P1: $\eta(z) = \eta_0$.
- P2: $\eta(z) = \eta_0 + \eta_1 z$.
- P3: $\eta(z) = \eta_0 + \eta_1 \frac{z}{1+z}$.

¹<http://github.com/dscolnic/Pantheon>

- P4: $\eta(z) = \eta_0 + \eta_1 \ln(1 + z)$.

We included these to study the impact of different characterizations on the analysis. The motivation for this form of parametrizations comes from the commonly used parametrizations for the equation of state parameter, viz. the Chevallier-Polarski-Linder (CPL) Parametrization, Jassal-Bagla-Padmanabhan (JBP) Parametrization etc [78–80].

In the first parametrization, we are choosing η to be redshift independent. In second parametrization, it is a simple Taylor series expansion around $z = 0$ but is not well behaved at higher z values. The third and fourth parametrizations are taken as these are well behaved even at high redshifts and are somewhat more slowly varying as compared to the second one.

Further in each parametrization of $\eta(z)$, we discuss two cases. In the first case we choose a flat universe by considering $\Omega_{k0} = 0$ and then put constraints on M_B and η . In the second case, we consider Ω_{k0} as a free parameter corresponding to a non-flat universe.

Part II: Test of variability of SNe Type Ia absolute luminosity

After testing the validity of CDDR in Part I, we solely focus on the variability of absolute magnitude of SNe Type Ia and use the following parametrizations of M_B

- M1: $M_B(z) = M_{B0}$.
- M2: $M_B(z) = M_{B0} + M_{B1}z$.
- M3: $M_B(z) = M_{B0} + M_{B1} \frac{z}{1 + z}$.
- M4: $M_B(z) = M_{B0} + M_{B1} \ln(1 + z)$.

In each parametrization of $M_B(z)$, we discuss two cases. In the first case we choose a flat universe and then put constraints on M_B and in the second case, we consider a non-flat universe.

We use **emcee**, a Python based package, to perform the Markov Chain Monte Carlo (MCMC) analysis [81]. We find the best fit of all parameters and once the MCMC method is performed, the confidence level with their 1σ , 2σ and 3σ uncertainties are computed with the Python package **corner**[82].

In this work, we assume a broad flat prior for all parameters (Table 1). We use 100 walkers which take 10000 steps for exploring the parameter space with MCMC chains. The first 10% of the steps are discarded as burn-in period and the posterior distributions are analysed based on the remaining samples. To ensure that the chains are converging, an auto-correlation study is performed. For this we compute the integrated auto-correlation time τ_f using the *autocorr.integrated.time* function of the **emcee** package. For more details, please see ref.[81].

Parameter	Prior Range
M_B	U[-21,-17]
η_0	U[-3,3]
η_1	U[-2,2]
Ω_{k0}	U[-2.5,2.5]

Table 1: The prior range of M_B , η_0 , η_1 and Ω_{k0} .

4 Results

In this paper our aim is to probe the variation of the absolute luminosity (M_B) of SNe Type Ia. This paper is divided into two parts. In the first part, we propose a new (cosmological) model-independent test for CDDR by using SNe Type Ia observations and $H(z)$ measurements from cosmic chronometers. In the second part we assume that CDDR is valid and check the dependency of absolute magnitude on redshift.

4.1 Test of CDDR

In this part, we consider the distance duality parameter (η) and take into account four parametrizations of $\eta(z)$. In each parametrization, we discuss two cases- flat and non-flat universe.

P1. $\eta(z) = \eta_0$.

Taking $\eta(z)$ to be a constant, the best fit values of M_B , η_0 and Ω_{k0} parameters are given in Table 2.

Parameter	Flat Universe	Non-Flat Universe
M_B	$-19.300^{+0.812}_{-0.874}$	$-19.653^{+0.587}_{-0.431}$
η_0	$0.960^{+0.300}_{-0.476}$	$1.124^{+0.250}_{-0.265}$
Ω_{k0}	—	$0.076^{+0.110}_{-0.106}$

Table 2: The best fit values of M_B , η_0 and Ω_{k0} with 1σ confidence level for P1 parametrization.

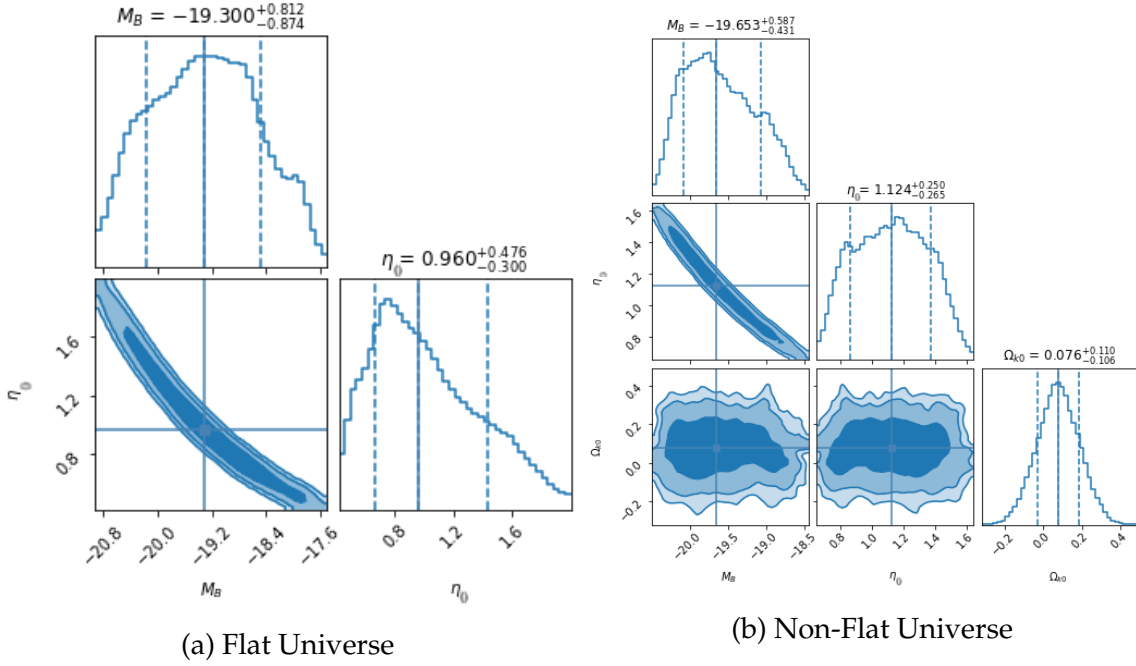


Figure 3: The 1D and 2D posterior distributions of M_B, η_0 and Ω_{k0} for P1 parametrization.

The best fit value of $\eta(z)$ shown in Table 2 for both flat as well as non-flat universe, indicates that the cosmic distance duality relation ($\eta(z) = 1$) holds at 1σ confidence level. In both flat and non-flat case, the value of M_B remains same within 1σ confidence level which reflects that M_B doesn't have any strong dependence on the curvature parameter. The 1D and 2D posterior distributions of M_B, η_0 and Ω_{k0} with $1\sigma, 2\sigma$ and 3σ confidence levels for flat and non-flat universe are shown in Fig.3. The contour plots shown in Fig.3 indicate a negative correlation between M_B and η_0 . Further, this parametrization supports a flat universe within 1σ confidence level.

P2. $\eta(z) = \eta_0 + \eta_1 z$.

In this parametrization, we consider $\eta(z)$ as a function of redshift. The best fit values of M_B, η_0, η_1 and Ω_{k0} are given in Table 3.

In case of a flat universe, the best fit value of η_1 , suggests that the cosmic distance duality parameter holds within 1σ confidence level. Similarly in the case of a non-flat universe, there is no violation of cosmic distance duality relation at 3σ confidence level. The obtained value of Ω_{k0} can accommodate a flat universe at 3σ confidence level. The best fit values of M_B in both a flat universe and a non-flat universe remain the same within 1σ confidence level which indicates that there is no strong impact of Ω_{k0} on M_B .

The 1D and 2D posterior distributions of M_B, η_0, η_1 and Ω_{k0} in both flat and non-flat universes are shown in Fig. 4. The 2D posterior plots for two cases (flat and

Parameter	Flat Universe	Non-Flat Universe
M_B	$-19.254^{+0.616}_{-0.778}$	$-19.574^{+0.518}_{-0.495}$
η_0	$0.938^{+0.405}_{-0.232}$	$1.097^{+0.279}_{-0.234}$
η_1	$0.002^{+0.010}_{-0.009}$	$-0.098^{+0.047}_{-0.049}$
Ω_{k0}	—	$1.108^{+0.503}_{-0.531}$

Table 3: The best fit values of M_B , η_0 , η_1 and Ω_{k0} with 1σ confidence level for P2 parametrization.

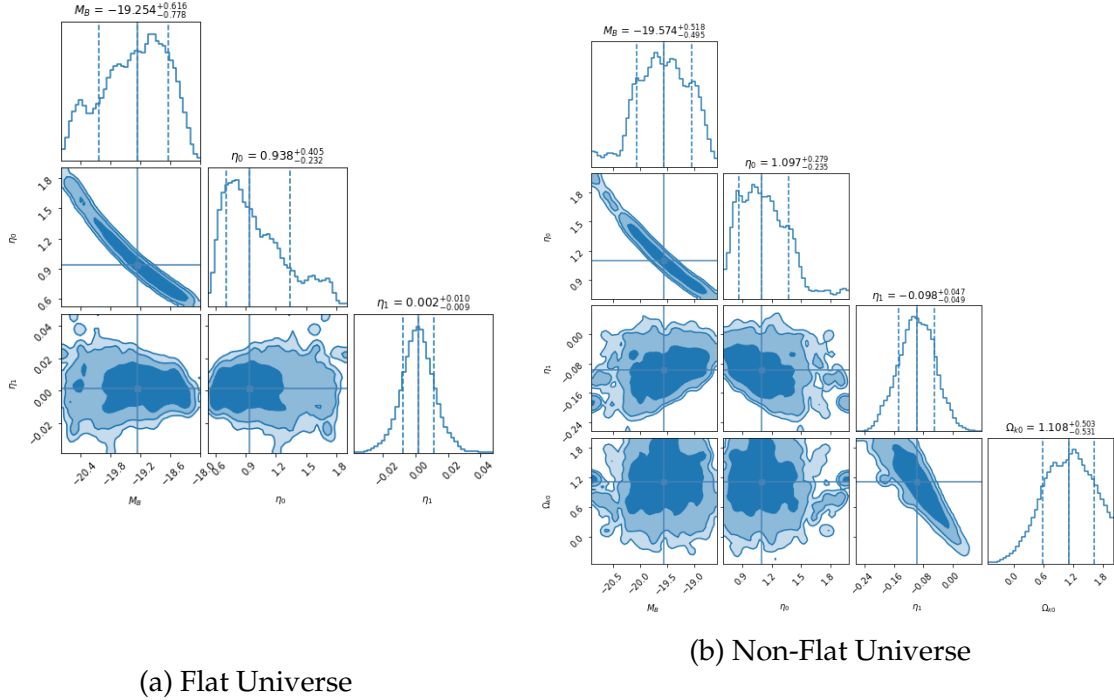


Figure 4: The 1D and 2D posterior distributions of M_B , η_0 , η_1 and Ω_{k0} for P2 parametrization.

non-flat) show a correlation between M_B and distance duality parameters.

P3. $\eta(z) = \eta_0 + \eta_1 \frac{z}{1+z}$.

In this parametrization, we choose η as a function of redshift which converges at high redshift. The best fit values of M_B , η_0 , η_1 and Ω_{k0} are given in Table 4.

In a flat universe, the CDDR holds within 1σ confidence level. Even, for the non-flat universe, results indicate that CDDR holds true at 2σ confidence level. The best fit value of Ω_{k0} prefer a flat universe at 2σ confidence level. The best fit values of M_B in both a flat universe and a non-flat universe at 1σ confidence level indicates that there is no strong correlation between Ω_{k0} and M_B .

Parameter	Flat Universe	Non-Flat Universe
M_B	$-19.342^{+0.489}_{-0.369}$	$-19.368^{+0.432}_{-0.335}$
η_0	$0.976^{+0.179}_{-0.197}$	$0.993^{+0.166}_{-0.178}$
η_1	$0.003^{+0.015}_{-0.015}$	$-0.047^{+0.036}_{-0.031}$
Ω_{k0}	—	$0.312^{+0.194}_{-0.204}$

Table 4: The best fit values of M_B , η_0 , η_1 and Ω_{k0} with 1σ confidence level for P3 parametrization.

The 1D and 2D posterior distributions of M_B , η_0 , η_1 and Ω_{k0} for P3 parametrization of Part I are shown in Fig. 5. This figure shows strong correlation between M_B and η_0 , and Ω_{k0} and η_1 .

P4. $\eta(z) = \eta_0 + \eta_1 \ln(1 + z)$.

In this parametrization, we choose η as a function of redshift which varies with redshift logarithmic. The best fit value of M_B , η_0 , η_1 and Ω_{k0} are given in Table 5.

In a flat universe, the best fit value of $\eta(z)$ supports the validity of CDDR at 1σ confidence level. Similarly, the results in a non-flat universe indicate that CDDR does hold true at 2σ confidence level. We find the best fit value of Ω_{k0} a flat universe at 2σ confidence level. The best fit values of M_B in both a flat universe and a non-flat universe indicate that there is no strong correlation between Ω_{k0} and M_B at 1σ confidence level.

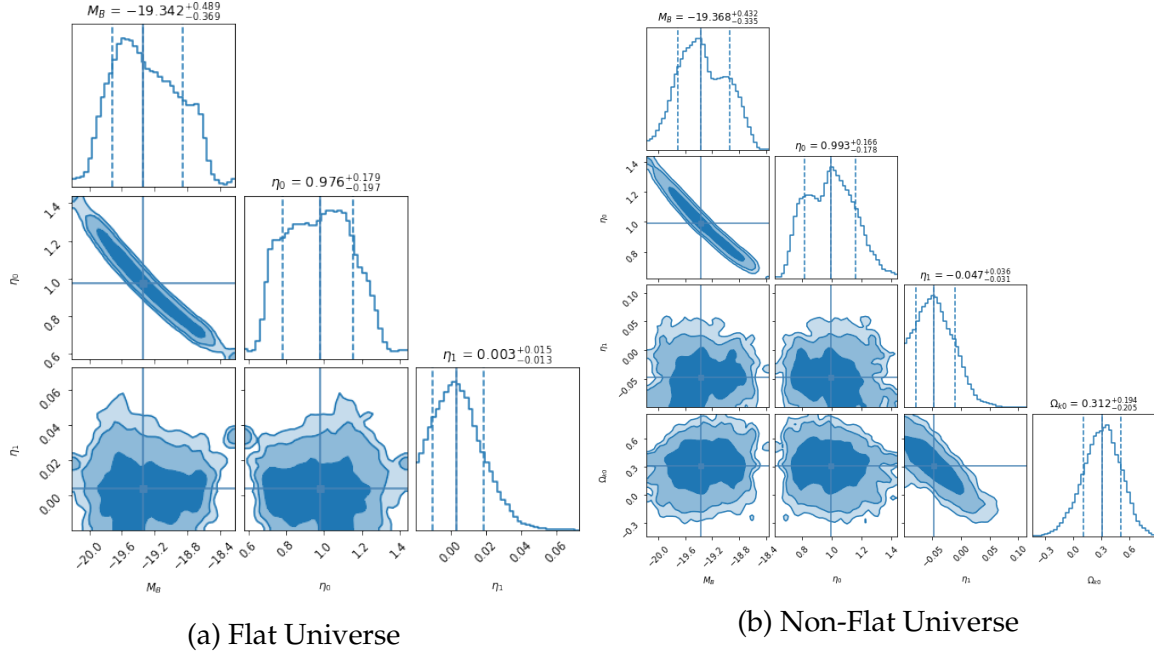


Figure 5: The 1D and 2D posterior distributions of M_B , η_0 , η_1 and Ω_{k0} for P3 parametrization.

Parameter	Flat Universe	Non-Flat Universe
M_B	$-19.202^{+0.469}_{-0.505}$	$-20.000^{+0.582}_{-0.402}$
η_0	$0.916^{+0.241}_{-0.178}$	$1.327^{+0.265}_{-0.306}$
η_1	$0.003^{+0.014}_{-0.012}$	$-0.046^{+0.041}_{-0.032}$
Ω_{k0}	—	$0.333^{+0.215}_{-0.243}$

Table 5: The best fit values of M_B , η_0 , η_1 and Ω_{k0} with 1σ confidence level for P4 parametrization.

The 1D and 2D posterior distributions of M_B , η_0 , η_1 and Ω_{k0} for P4 parametrization are shown in Fig. 6. This figure shows strong correlation between M_B and η_0 , and Ω_{k0} and η_1 .

4.2 Test of variability of SNe Type Ia absolute luminosity

In the first part, we find that the cosmic distance duality relation is not violated at 2σ confidence level in four parametrizations of $\eta(z)$ (P1, P2, P3 and P4).

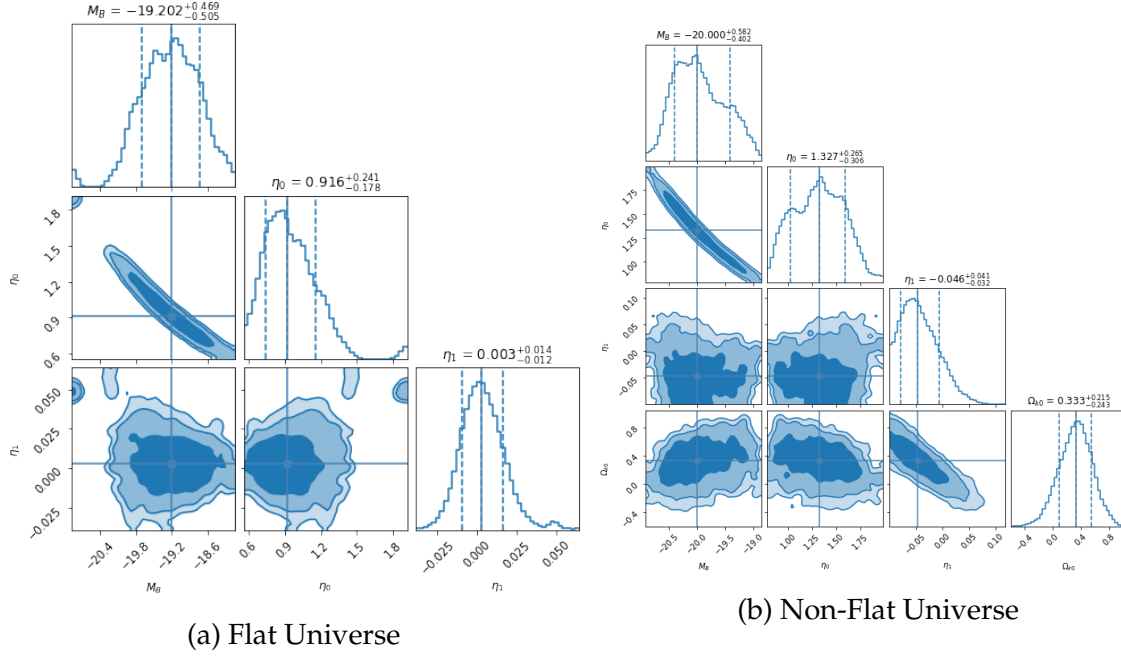


Figure 6: The 1D and 2D posterior distributions of M_B , η_0 , η_1 and Ω_{k0} for P4 parametrization.

Therefore, in this part we consider that the CDDR is valid and to check the dependency of absolute magnitude on redshift, we vary M_B with redshift in four different ways in both a flat and a non-flat universe.

M1: $M_B(z) = M_{B0}$.

In the first parametrization of M_B we consider it as a constant parameter. The best fit values of M_B and Ω_{k0} parameters are given in Table 6.

Parameter	Flat Universe	Non-Flat Universe
M_{B0}	$-19.390^{+0.015}_{-0.015}$	$-19.393^{+0.015}_{-0.015}$
Ω_{k0}	—	$0.075^{+0.104}_{-0.103}$

Table 6: The best fit values of M_{B0} and Ω_{k0} with 1σ confidence level for M1 parametrization.

From table 6, we find that the best fit value of M_B is the same in both flat and non-flat universes within 1σ confidence level. Further, the best fit value of $\Omega_{k0} = 0.075^{+0.104}_{-0.103}$ suggests a flat universe at 1σ confidence level.

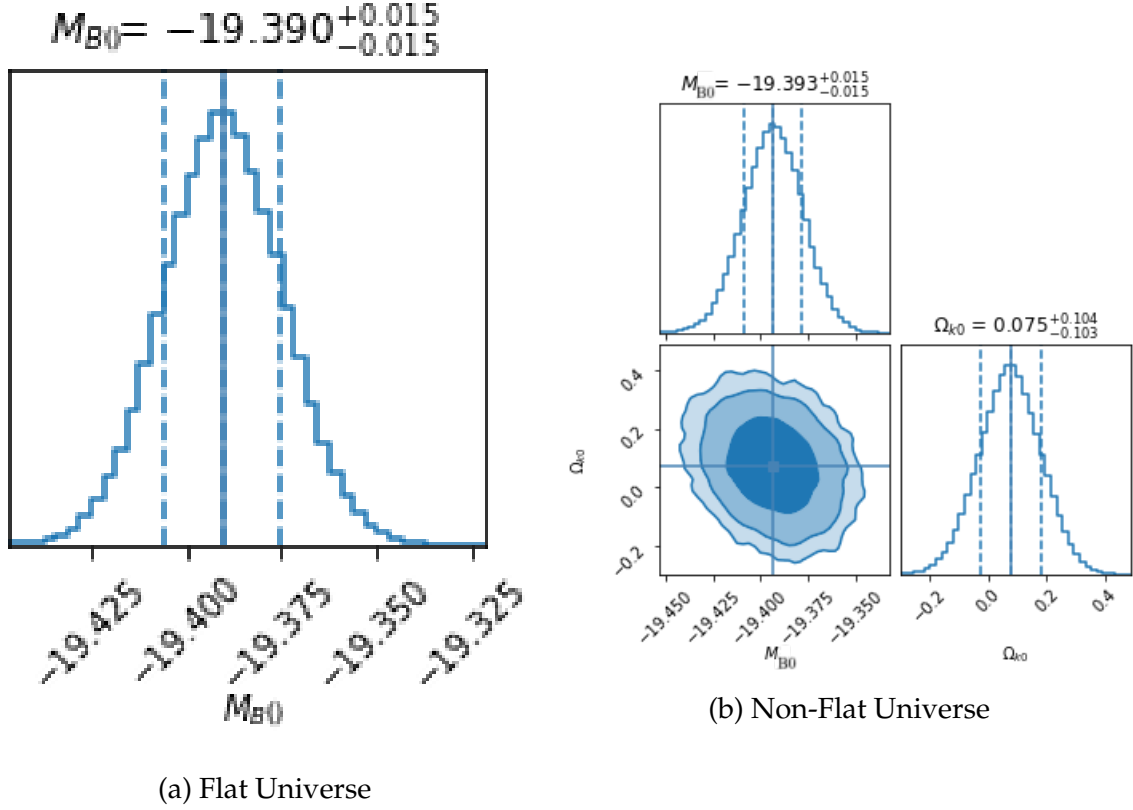


Figure 7: The 1D and 2D posterior distributions of M_{B0} and Ω_{k0} for M1 parametrization.

The 1D and 2D posterior distributions of M_B and Ω_{k0} for M1 parametrization are shown in Fig. 7. This figure shows that there is no correlation between M_B and Ω_{k0} .

M2: $M_B(z) = M_{B0} + M_{B1}z$.

In this parametrization, we consider M_B as a function of redshift. The best fit values of M_{B0} , M_{B1} and Ω_{k0} are given in Table 7.

In case of a flat universe, we don't find any signal of the redshift evolution of absolute magnitude with 1σ confidence level. Similarly, in a non-flat universe, there is no redshift dependence of the absolute magnitude at 2σ confidence level. Further, the result supports a flat universe at 2σ confidence level.

Figure 8 illustrates the 1D and 2D posterior distributions of M_{B0} , M_{B1} and Ω_{k0} for M2 parametrization. In this figure, the plot for a non-flat universe indicates a mild correlation between absolute magnitude and cosmic curvature parameter.

Parameter	Flat Universe	Non-Flat Universe
M_{B0}	$-19.391^{+0.016}_{-0.016}$	$-19.376^{+0.018}_{-0.019}$
M_{B1}	$0.005^{+0.021}_{-0.021}$	$-0.152^{+0.089}_{-0.091}$
Ω_{k0}	—	$0.823^{+0.471}_{-0.450}$

Table 7: The best fit values of M_{B0} , M_{B1} and Ω_{k0} with 1σ confidence level for M2 parametrization.

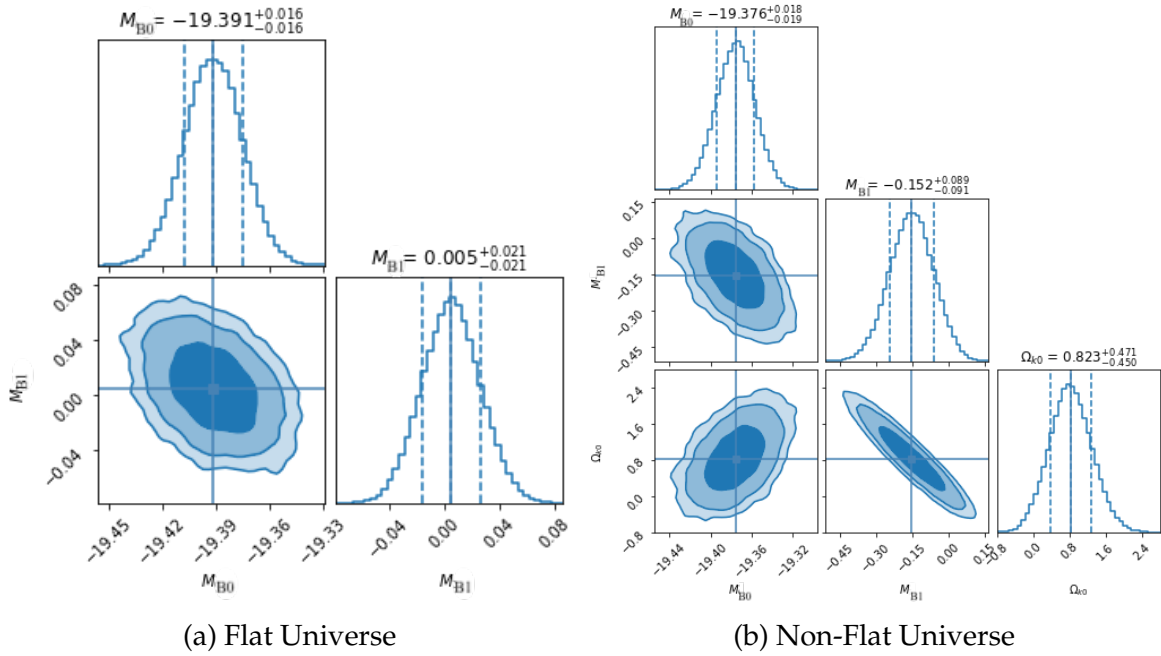


Figure 8: The 1D and 2D posterior distributions of M_{B0} , M_{B1} and Ω_{k0} for M2 parametrization.

M3: $M_B(z) = M_{B0} + M_{B1} \frac{z}{1+z}$.

In this parametrization, we choose M_B as a function of redshift which converges at high redshift. The best fit values of M_{B0} , M_{B1} and Ω_{k0} are given in Table 8.

In this parametrization, the best fit value of M_{B1} in both a flat and a non-flat universe suggests that the absolute magnitude does not evolve with redshift at 2σ confidence level. Furthermore, there is no indication of deviation from flat universe at 2σ confidence level yet it mildly supports a non flat universe.

In both flat and non-flat universes, the 1D and 2D posterior distributions of M_{B0} , M_{B1} and Ω_{k0} are illustrated in Figure 9. The plot for non-flat universe indicates

Parameter	Flat Universe	Non-Flat Universe
M_{B0}	$-19.390^{+0.017}_{-0.017}$	$-19.380^{+0.018}_{-0.018}$
M_{B1}	$0.001^{+0.038}_{-0.040}$	$-0.111^{+0.082}_{-0.083}$
Ω_{k0}	—	$0.343^{+0.214}_{-0.225}$

Table 8: The best fit values of M_{B0} , M_{B1} and Ω_{k0} with 1σ confidence level for M3 parametrization.

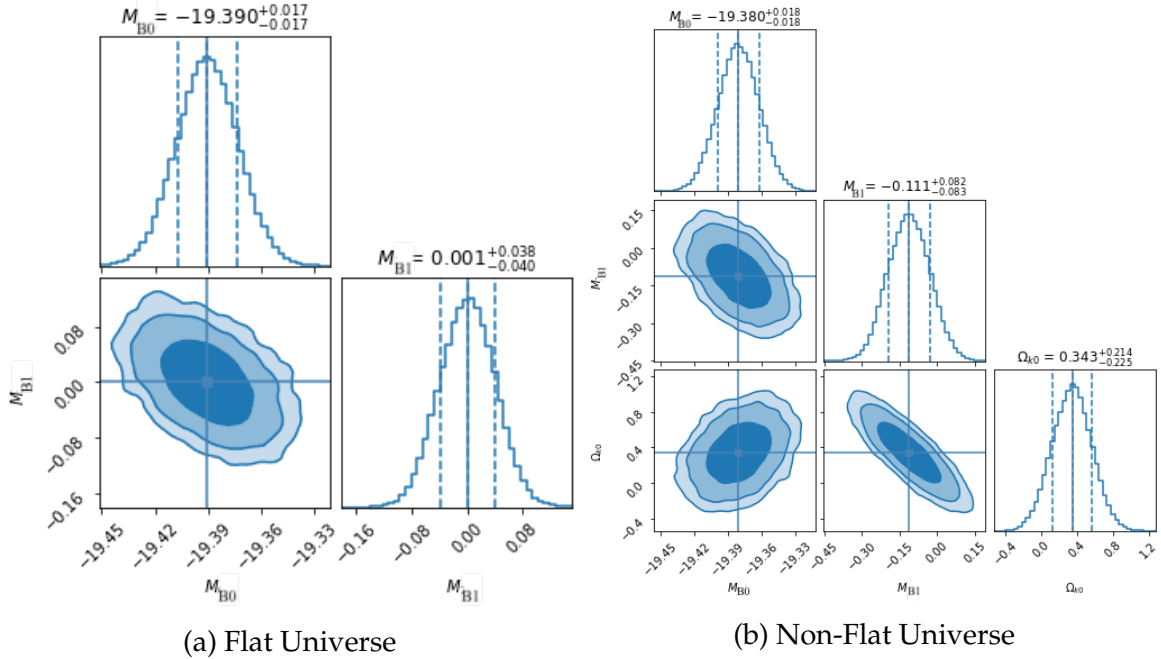


Figure 9: The 1D and 2D posterior distributions of M_{B0} , M_{B1} and Ω_{k0} for M3 parametrization.

a correlation between absolute magnitude and cosmic curvature parameter.

M4: $M_B(z) = M_{B0} + M_{B1} \ln(1+z)$.

In this last parametrization, we choose M_B as a logarithmic function of redshift. The best fit values of M_{B0} , M_{B1} and Ω_{k0} are given in Table 9.

In this parametrization, for both a flat and a non-flat universe, the absolute magnitude does not evolve with redshift at 2σ confidence level. Furthermore, the best fit value of Ω_{k0} supports a flat universe at 2σ confidence level.

In both flat and non-flat universes, the 1D and 2D posterior distributions of

Parameter	Flat Universe	Non-Flat Universe
M_{B0}	$-19.391^{+0.017}_{-0.016}$	$-19.380^{+0.017}_{-0.018}$
M_{B1}	$0.005^{+0.030}_{-0.029}$	$-0.110^{+0.079}_{-0.078}$
Ω_{k0}	—	$0.442^{+0.282}_{-0.287}$

Table 9: The best fit values of M_{B0} , M_{B1} and Ω_{k0} with 1σ confidence level for M4 parametrization.

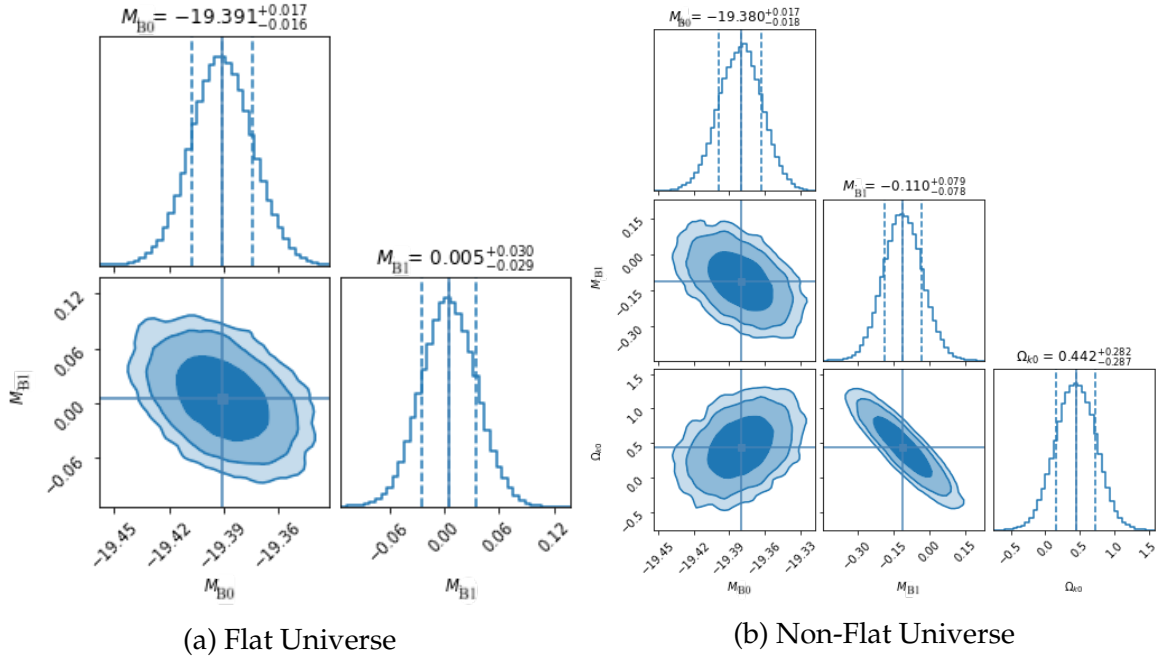


Figure 10: The 1D and 2D posterior distributions of M_{B0} , M_{B1} and Ω_{k0} for M4 parametrization.

M_{B0} , M_{B1} and Ω_{k0} are illustrated in Figure 10. The plot for non-flat universe indicates a correlation between absolute magnitude and cosmic curvature parameter.

5 Discussion and Conclusions

In this work, we test the validity of the cosmic distance duality relation which relates the luminosity distance to angular diameter distance via redshift. We use the recent database of 1048 Type Ia supernovae named Pantheon for the luminosity distance. For the angular diameter distance, we first reconstruct the Hubble parameter, $H(z)$ database of 31 datapoints from Cosmic Chronometers in a model-independent way

using the Gaussian Process. Then by adopting the Planck prior on $H_0 = 67.66 \pm 0.42 \text{ km s}^{-1} \text{ Mpc}^{-1}$, the angular diameter distance is obtained corresponding to the reconstructed $H(z)$. Further, in the luminosity distance we have a free parameter, i.e. absolute magnitude of Type Ia supernovae (M_B), and we put constraints on it simultaneously with other cosmological parameters i.e. Ω_{k0} and $\eta(z)$. Finally, we allow M_B and $\eta(z)$ to evolve with redshift to check whether these are constant quantities or evolve with cosmic time.

We divide this work into two parts as follows.

(A) Part I: Test of CDDR

In this part, we do not assume that cosmic distance duality is valid and to test this, we consider a free parameter i.e. $\eta(z)$. We fit this parameter simultaneously with M_B and Ω_{k0} . To check the dependency of the distance duality parameter on redshift, we assume four parametrizations of $\eta(z)$. A brief summary of the results is as follows:

- In the case of a flat universe, all parametrizations suggest that the cosmic distance duality relation holds at 1σ confidence level.
- For the non-flat universe, P1, supports the $\eta(z) = 1$ at 1σ confidence level, P3 & P4 parametrizations at 2σ confidence level and, P2 parametrization at 3σ confidence level. For this case, this variation in the confidence level for the validity of $\eta(z) = 1$ directly indicates the correlation between the $\eta(z)$ and Ω_{k0} . This analysis also highlights that the results are sensitive to the choice of parametrization and hence, it justifies our use of multiple parametrizations.
- Consistently, for flat and non-flat cases, all the 2D contours between η_0 and M_B in Part I of the analysis indicate a very strong negative correlation. This points to the need of considering the validity of cosmic distance duality relation in Part II to independently probe the variability of the absolute magnitude M_B .
- In non-flat universe case, the parametrization, P1, strongly suggests a flat universe within 1σ confidence level while parametrization P2, P3 and P4 also supports the flat universe within 2σ confidence level. Though the best fit value of Ω_{k0} mildly prefer a non-flat universe.

(B) Part II: Test of variability of SNe Type Ia absolute luminosity

In the second part we assume that the cosmic distance duality relation is valid, i.e. $\eta=1$. We are thus left with two parameters that we have to fit simultaneously. These

parameters are M_B and Ω_{k0} . To test the dependency of M_B on redshift, we consider four parametrizations of M_B . All four parametrizations have two model parameters M_{B0} and, M_{B1} . While analysing we choose M_{B0} to be constrained in the uniform prior range $U[-21, -17]$ and, M_{B1} in the uniform prior range $U[-2, +2]$. In each parametrization, we discuss two cases. In the first case we consider a flat universe i.e. $\Omega_{k0} = 0$ and in the second case we choose a non-flat universe.

Our main conclusions of this part are listed below:

- In the flat universe case, the parametrization M1, M2 and, M4, support no evolution of absolute magnitude with redshift with 1σ confidence level. Even for the parametrization M3, our analysis does not show any signal of redshift evolution of absolute magnitude at 2σ confidence level.
- Similarly, in the non-flat universe case, for all parametrizations, no redshift evolution has been found in our analysis in absolute luminosity M_B at 2σ confidence level. Hence from our analysis in Part I and Part II, we don't find any indication towards a statistically significant variability of absolute magnitude (M_B) of type Ia supernova.
- For all parametrizations of the absolute magnitude M_B , the best fit value of Ω_{k0} suggests a flat universe at 2σ confidence level. However, in the parametrizations M2, M3 and M4, the best fit value of Ω_{k0} show mild preference for a non-flat universe. Further, from the 1D and 2D contours of all four parametrizations of $M_B(z)$ for non-flat case, we observed a negative correlation between the absolute magnitude and cosmic curvature which should be analysed further.

It is important to note that in Part I, we fit the distance duality parameter $\eta(z)$ along with M_B and Ω_{k0} . On the other hand, in Part II we assume the validity of the cosmic distance duality relation i.e; $\eta(z) = 1$ and are thus left with only M_B & Ω_{k0} as free parameters. Thus, the number of free parameters to be probed decreases from four in Part I to three in Part II. In Part I, our analysis suggests a strong correlation between the $\eta(z)$ and M_B values, which seems to have an impact on the 1σ error bars of M_B . However, in Part II, the $\eta(z)$ parameter has been excluded, hence it results in tighter 1σ constraints on M_B . This correlation between $\eta(z)$ and M_B has also been highlighted using BAO and Cluster observations as well [83].

(C) Impact of different prior values of Hubble Parameter (H_0)

In this analysis, we consider the Planck prior and discuss our results in two parts. In the first part we test the CDDR and in the second part we test the evolution of M_B . However, it is important to check whether our results are sensitive to the chosen prior of H_0 or not. To check this sensitivity on the chosen prior for H_0 , we make two

more prior choices of H_0 while reconstructing the angular diameter distance. These two priors are

- No Prior on H_0 . The reconstructed H_0 value using GP is $67.64 \pm 4.79 \text{ km s}^{-1} \text{Mpc}^{-1}$.
- Planck Prior on $H_0 = 67.66 \pm 0.42 \text{ km s}^{-1} \text{Mpc}^{-1}$
- SH0ES Prior on $H_0 = 73.20 \pm 1.30 \text{ km s}^{-1} \text{Mpc}^{-1}$.

To check the impact of the prior in our analysis, we repeat the whole analysis for all parametrizations of $\eta(z)$ and M_B with the three priors of H_0 i.e. No prior, Planck prior and SH0ES prior [84]. In Table 10 and Table 11, we show the results only for the third parametrization of $\eta(z)$ (i.e $P3$) and $M_B(z)$ (i.e. $M3$) just to show their behaviour with different priors. The remaining parametrizations in all three priors of H_0 give the same conclusions as we find here in Table 10 and Table 11.

Parameter	No Prior	Planck Prior	SH0ES Prior
Case.1 Flat Universe			
M_B	$-19.161^{+0.694}_{-0.590}$	$-19.342^{+0.489}_{-0.369}$	$-19.038^{+0.514}_{-0.454}$
η_0	$0.927^{+0.265}_{-0.254}$	$0.976^{+0.179}_{-0.197}$	$0.910^{+0.206}_{-0.193}$
η_1	$-0.016^{+0.008}_{-0.003}$	$0.003^{+0.015}_{-0.015}$	$-0.105^{+0.022}_{-0.031}$
Case.2 Non-Flat Universe			
M_B	$-19.493^{+0.433}_{-0.439}$	$-19.368^{+0.432}_{-0.335}$	$-19.133^{+0.563}_{-0.484}$
η_0	$1.085^{+0.256}_{-0.196}$	$0.993^{+0.166}_{-0.178}$	$0.948^{+0.226}_{-0.217}$
η_1	$-0.077^{+0.024}_{-0.016}$	$-0.047^{+0.036}_{-0.031}$	$-0.089^{+0.017}_{-0.008}$
Ω_{k0}	$0.132^{+0.152}_{-0.149}$	$0.312^{+0.194}_{-0.204}$	$-0.029^{+0.135}_{-0.135}$

Table 10: The best fit values of M_B , η_0 , η_1 and Ω_{k0} with 1σ confidence level for three H_0 priors for $P3$ parametrization of Part I.

Through careful analysis, we find that while reconstructing the $H(z)$ data, the choice of the prior value of H_0 does not make a significant impact on correlations among the parameters.

We also notice that the 1σ error bars of the M_B also get affected by the uncertainties of the H_0 prior chosen for the analysis. For example, the uncertainty in the value

Parameter	No Prior	Planck Prior	SH0ES Prior
Case.1 Flat Universe			
M_{B0}	$-19.300^{+0.150}_{-0.155}$	$-19.390^{+0.017}_{-0.017}$	$-19.241^{+0.039}_{-0.039}$
M_{B1}	$-0.130^{+0.040}_{-0.040}$	$0.001^{+0.038}_{-0.040}$	$-0.268^{+0.040}_{-0.040}$
Case.2 Non-Flat Universe			
M_{B0}	$-19.286^{+0.147}_{-0.167}$	$-19.380^{+0.018}_{-0.018}$	$-19.229^{+0.039}_{-0.039}$
M_{B1}	$-0.238^{+0.079}_{-0.078}$	$-0.111^{+0.082}_{-0.083}$	$-0.407^{+0.079}_{-0.080}$
Ω_{k0}	$0.342^{+0.213}_{-0.213}$	$0.343^{+0.214}_{-0.225}$	$0.382^{+0.192}_{-0.183}$

Table 11: The best fit values of M_{B0} , M_{B1} and Ω_{k0} with 1σ confidence level for three H_0 priors for M3 parametrization of Part II.

of H_0 from CMB is 0.42 while that from SH0ES is 1.3. We find that in the case of using the CMB prior on H_0 , the error bars of M_B are much smaller as compared to those obtained by using the SH0ES prior. It seems that the uncertainty in the prior propagates in M_B during the fitting analysis and affects the error bars of M_B . Similar to cosmic probes like Cosmic Chronometers and Supernovae Type Ia, other independent probes like strong gravitational lensing (Time Delay angular distance measure) have also seen that the M_B values and error bars are impacted by the associated uncertainties in the input priors, data and parameter values [85]. Given the above mentioned observations, we can conclude that along with the consideration of the $\eta(z)$ parameter, the uncertainties in the prior value of H_0 also impacts the 1σ bounds on the M_B .

Finally, we observe that even if we adopt different priors for H_0 , the absolute magnitude of SNe Type Ia does not show any redshift dependence in both flat and non-flat universes. This is consistent with the expected non-variability of M_B up to 3σ confidence level and shows no deviation from the observationally expected assumptions. Though our analysis supports a flat universe but we observed the mild preference of best fit value of Ω_{k0} towards a non flat universe. It should be noted that there is a strong correlation between the absolute magnitude, the distance duality parameter. In Part II, we observed mild correlation between absolute magnitude and cosmic curvature as well. Any signal of deviation in one of these parameters will impact the rest of the parameters and the underlying assumptions. We expect that one can resolve these correlations among different parameters by performing a

similar analysis with a larger data set of Supernovae and other observational probes. Upcoming surveys such as the Large Synoptic Survey, the Wide Field Infrared Survey and survey from Large Synoptic Survey Telescope (LSST) may assist us in detecting any deviations from the standard supernova type Ia light-curve modeling as well as deviation from the standard cosmological model, i.e. the Λ CDM model [86–89].

Acknowledgements

We are grateful to the anonymous reviewer for her/his very enlightening remarks which have helped improve the paper. Darshan Kumar is supported by an INSPIRE Fellowship under the reference number: IF180293, DST India. A.R. and Darshan Kumar acknowledges facilities provided by the IUCAA Centre for Astronomy Research and Development (ICARD), University of Delhi. In this work some of the figures were created with `numpy` [90] and `matplotlib` [91] Python modules.

Bibliography

- [1] A. G. Riess *et al.* *Observational Evidence from Supernovae for an Accelerating Universe and a Cosmological Constant.* *AJ*, **116**, 1009, (1998).
- [2] S. Perlmutter *et al.* *Measurements of Ω and Λ from 42 High-Redshift Supernovae.* *ApJ*, **517**, 565, (1999).
- [3] P. J. Peebles and B. Ratra. *The cosmological constant and dark energy.* *Rev. Mod. Phys.*, **75**, 559, (2003).
- [4] R. R. Caldwell and M. Kamionkowski. *The Physics of Cosmic Acceleration.* *Annu. Rev. Nucl. Part. Sci.*, **59**, 397, (2009).
- [5] D. H. Weinberg, M. J. Mortonson, D. J. Eisenstein, C. Hirata, A. G. Riess and E. Rozo. *Observational probes of cosmic acceleration.* *Phys. Rep.*, **530**, 87, (2013).
- [6] W. Hillebrandt and J. C. Niemeyer. *Type Ia Supernova Explosion Models.* *Annu. Rev. Astron. Astrophys.*, **38**, 191, (2000).
- [7] M. M. Phillips. *The Absolute Magnitudes of Type IA Supernovae.* *ApJ*, **413**, L105, (1993).
- [8] R. Tripp. *A two-parameter luminosity correction for Type IA supernovae.* *A&A*, **331**, 815, (1998).
- [9] S. Jha, A. G. Riess and R. P. Kirshner. *Improved Distances to Type Ia Supernovae with Multicolor Light-Curve Shapes: MLCS2k2.* *ApJ*, **659**, 122, (2007).
- [10] J. Guy *et al.* *SALT2: using distant supernovae to improve the use of type Ia supernovae as distance indicators.* *A&A*, **466**, 11, (2007).
- [11] A. Conley *et al.* *SiFTO: An Empirical Method for Fitting SN Ia Light Curves.* *ApJ*, **681**, 482–498, (2008).
- [12] W. Zheng and A. V. Filippenko. *An Empirical Fitting Method for Type Ia Supernova Light Curves: A Case Study of SN 2011fe.* *ApJ*, **838**, L4, (2017).

- [13] D. M. Scolnic et al. *The Complete Light-curve Sample of Spectroscopically Confirmed SNe Ia from Pan-STARRS1 and Cosmological Constraints from the Combined Pantheon Sample*. *ApJ*, **859**, 101, (2018).
- [14] M. Childress et al. *Host Galaxy Properties and Hubble Residuals of Type Ia Supernovae from the Nearby Supernova Factory*. *ApJ*, **770**, 108, (2013).
- [15] Y.-L. Kim, Y. Kang and Y.-W. Lee. *Environmental Dependence of Type Ia Supernova Luminosities from the YONSEI Supernova Catalog*. *J. Korean Astron. Soc.*, **52**, 181, (2019).
- [16] J. S. Gallagher, P. M. Garnavich, N. Caldwell, R. P. Kirshner, S. W. Jha, W. Li, M. Ganeshalingam and A. V. Filippenko. *Supernovae in Early-Type Galaxies: Directly Connecting Age and Metallicity with Type Ia Luminosity*. *ApJ*, **685**, 752, (2008).
- [17] M. Hamuy, S. C. Trager, P. A. Pinto, M. M. Phillips, R. A. Schommer, V. Ivanov and N. B. Suntzeff. *A Search for Environmental Effects on Type Ia Supernovae*. *AJ*, **120**, 1479, (2000).
- [18] B. S. Wright and B. Li. *Type Ia supernovae, standardizable candles, and gravity*. *Phys. Rev. D*, **97**, 083505, (2018).
- [19] P. S. Drell, T. J. Loredo and I. Wasserman. *Type Ia Supernovae, Evolution, and the Cosmological Constant*. *ApJ*, **530**, 593, (2000).
- [20] F. Combes. *Properties of SN-host galaxies*. *New Astron. Rev.*, **48**, 583, (2004).
- [21] I. Zehavi, A. G. Riess, R. P. Kirshner and A. Dekel. *A Local Hubble Bubble from Type Ia Supernovae?* *ApJ*, **503**, 483, (1998).
- [22] A. Conley, R. G. Carlberg, J. Guy, D. A. Howell, S. Jha, A. G. Riess and M. Sullivan. *Is There Evidence for a Hubble Bubble? The Nature of Type Ia Supernova Colors and Dust in External Galaxies*. *ApJ*, **664**, L13, (2007).
- [23] M. Ishak, A. Upadhye and D. N. Spergel. *Probing cosmic acceleration beyond the equation of state: Distinguishing between dark energy and modified gravity models*. *Phys. Rev. D*, **74**, 043513, (2006).
- [24] M. Kunz and D. Sapone. *Dark Energy versus Modified Gravity*. *Phys. Rev. Lett.*, **98**, 121301, (2007).
- [25] E. Bertschinger and P. Zukin. *Distinguishing modified gravity from dark energy*. *Phys. Rev. D*, **78**, 024015, (2008).
- [26] A. Aguirre. *Intergalactic Dust and Observations of Type Ia Supernovae*. *ApJ*, **525**, 583, (1999).
- [27] M. Rowan-Robinson. *Do Type Ia supernovae prove $\Lambda > 0$?* *Mon. Not. Roy. Astron. Soc.*, **332**, 352, (2002).
- [28] A. Goobar, L. Bergström and E. Mörtzell. *Measuring the properties of extragalactic dust and implications for the Hubble diagram*. *A&A*, **384**, 1, (2002).
- [29] A. Goobar, S. Dhawan and D. Scolnic. *The cosmic transparency measured with Type Ia supernovae: implications for intergalactic dust*. *Mon. Not. Roy. Astron. Soc.*, **477**, L75, (2018).
- [30] A. Avgoustidis, L. Verde and R. Jimenez. *Consistency among distance measurements: transparency, BAO scale and accelerated expansion*. *JCAP*, **06**, 012, (2009).

- [31] A. Avgoustidis, C. Burrage, J. Redondo, L. Verde and R. Jimenez. *Constraints on cosmic opacity and beyond the standard model physics from cosmological distance measurements.* JCAP, **08**, 024, (2010).
- [32] I. Tutusaus, B. Lamine and A. Blanchard. *Model-independent cosmic acceleration and redshift-dependent intrinsic luminosity in type-Ia supernovae.* A&A, **625**, A15, (2019).
- [33] I. Tutusaus, B. Lamine, A. Dupays and A. Blanchard. *Is cosmic acceleration proven by local cosmological probes?* A&A, **602**, A73, (2017).
- [34] Y. Kang, Y.-W. Lee, Y.-L. Kim, C. Chung and C. H. Ree. *Early-type Host Galaxies of Type Ia Supernovae. II. Evidence for Luminosity Evolution in Supernova Cosmology.* ApJ, **889**, 8, (2020).
- [35] E. D. Valentino, S. Gariazzo, O. Mena and S. Vagnozzi. *Soundness of dark energy properties.* JCAP, **07**, 045, (2020).
- [36] D. Sapone, S. Nesseris and C. A. P. Bengaly. *Is there any measurable redshift dependence on the SN Ia absolute magnitude?* Phys. Dark Universe, **32**, 100814, (2021).
- [37] V. Vavryčuk. *Universe opacity and Type Ia supernova dimming.* Mon. Not. Roy. Astron. Soc., **489**, L63, (2019).
- [38] G. F. R. Ellis. *On the definition of distance in general relativity: I. M. H. Etherington (Philosophical Magazine ser. 7, vol. 15, 761 (1933)).* Gen. Relativ. Gravit., **39**, 1047, (2007).
- [39] R. F. L. Holanda, J. A. S. Lima and M. B. Ribeiro. *Testing the distance–duality relation with galaxy clusters and type Ia supernovae.* ApJ, **722**, L233, (2010).
- [40] J. A. S. Lima, J. V. Cunha and V. T. Zanchin. *Deformed Distance Duality Relations and Supernovae Dimming.* ApJ, **742**, L26, (2011).
- [41] Z. Li, P. Wu and H. Yu. *Cosmological-model-independent tests for the distance-duality relation from Galaxy Clusters and Type Ia Supernova.* ApJ, **729**, L14, (2011).
- [42] R. S. Gonçalves, R. F. L. Holanda and J. S. Alcaniz. *Testing the cosmic distance duality with X-ray gas mass fraction and supernovae data.* Mon. Not. Roy. Astron. Soc., **420**, L43, (2011).
- [43] X.-L. Meng, T.-J. Zhang, H. Zhan and X. Wang. *Morphology of Galaxy Clusters: A Cosmological Model-Independent Test of the Cosmic Distance-Duality Relation.* ApJ, **745**, 98, (2012).
- [44] R. F. L. Holanda, R. S. Gonçalves and J. S. Alcaniz. *A test for cosmic distance duality.* JCAP, **06**, 022, (2012).
- [45] X. Yang, H.-R. Yu, Z.-S. Zhang and T.-J. Zhang. *An improved method to test the distance-duality relation.* ApJ, **777**, L24, (2013).
- [46] N. Liang, Z. Li, P. Wu, S. Cao, K. Liao and Z.-H. Zhu. *A consistent test of the distance–duality relation with galaxy clusters and Type Ia Supernovae.* Mon. Not. Roy. Astron. Soc., **436**, 1017, (2013).
- [47] A. Shafieloo, S. Majumdar, V. Sahni and A. A. Starobinsky. *Searching for systematics in SNIa and galaxy cluster data using the cosmic duality relation.* JCAP, **04**, 042, (2013).
- [48] Y. Zhang. *Reconstruct the Distance Duality Relation by Gaussian Process.* arXiv:1408.3897, (2014).

- [49] S. S. da Costa, V. C. Busti and R. F. L. Holanda. *Two new tests to the distance duality relation with galaxy clusters*. JCAP, **10**, 061, (2015).
- [50] R. Nair, S. Jhingan and D. Jain. *Observational cosmology and the cosmic distance duality relation*. JCAP, **05**, 023, (2011).
- [51] Z. Chen, B. Zhou and X. Fu. *Testing the Distance-Duality Relation from Hubble, Galaxy Clusters and Type Ia Supernovae Data with Model Independent Methods*. Int. J. Theor. Phys., **55**, 1229, (2015).
- [52] R. F. L. Holanda, V. C. Busti and J. S. Alcaniz. *Probing the cosmic distance duality with strong gravitational lensing and supernovae Ia data*. JCAP, **02**, 054, (2016).
- [53] A. Rana, D. Jain, S. Mahajan and A. Mukherjee. *Revisiting the Distance Duality Relation using a non-parametric regression method*. JCAP, **07**, 026, (2016).
- [54] K. Liao, Z. Li, S. Cao, M. Biesiada, X. Zheng and Z.-H. Zhu. *The Distance Duality Relation from Strong Gravitational Lensing*. ApJ, **822**, 74, (2016).
- [55] R. F. L. Holanda and K. N. N. O. Barros. *Searching for cosmological signatures of the Einstein equivalence principle breaking*. Phys. Rev. D, **94**, 023524, (2016).
- [56] R. F. L. Holanda, S. H. Pereira and S. S. da Costa. *Searching for deviations from the general relativity theory with gas mass fraction of galaxy clusters and complementary probes*. Phys. Rev. D, **95**, 084006, (2017).
- [57] A. Rana, D. Jain, S. Mahajan, A. Mukherjee and R. F. L. Holanda. *Probing the cosmic distance duality relation using time delay lenses*. JCAP, **07**, 010, (2017).
- [58] H.-N. Lin, M.-H. Li and X. Li. *New constraints on the distance duality relation from the local data*. Mon. Not. Roy. Astron. Soc., **480**, 3117, (2018).
- [59] X. Fu, L. Zhou and J. Chen. *Testing the cosmic distance-duality relation from future gravitational wave standard sirens*. Phys. Rev. D, **99**, 083523, (2019).
- [60] C.-Z. Ruan, F. Melia and T.-J. Zhang. *Model-independent Test of the Cosmic Distance Duality Relation*. ApJ, **866**, 31, (2018).
- [61] R. F. L. Holanda, L. R. Colaço, S. H. Pereira and R. Silva. *Galaxy cluster Sunyaev-Zel'dovich effect scaling-relation and type Ia supernova observations as a test for the cosmic distance duality relation*. JCAP, **06**, 008, (2019).
- [62] J. Chen. *Testing the distance-duality relation with the baryon acoustic oscillations data and type Ia supernovae data*. Commun. Theor. Phys., **72**, 045401, (2020).
- [63] X. Zheng, K. Liao, M. Biesiada, S. Cao, T.-H. Liu and Z.-H. Zhu. *Multiple Measurements of Quasars Acting as Standard Probes: Exploring the Cosmic Distance Duality Relation at Higher Redshift*. ApJ, **892**, 103, (2020).
- [64] D. Kumar, D. Jain, S. Mahajan, A. Mukherjee and N. Rani. *Constraining cosmological and galaxy parameters using strong gravitational lensing systems*. Phys. Rev. D, **103**, 063511, (2021).
- [65] J. Hu and F. Y. Wang. *Testing the distance–duality relation in the $R_h = ct$ universe*. Mon. Not. Roy. Astron. Soc., **477**, 5064, (2018).
- [66] W. J. C. da Silva, R. F. L. Holanda and R. Silva. *Bayesian comparison of the cosmic duality scenarios*. Phys. Rev. D, **102**, 063513, (2020).

- [67] J. Magaña, M. H. Amante, M. A. Garcia-Aspeitia and V. Motta. *The Cardassian expansion revisited: constraints from updated Hubble parameter measurements and type Ia supernova data*. Mon. Not. Roy. Astron. Soc., **476**, 1036, (2018).
- [68] R. Jimenez and A. Loeb. *Constraining Cosmological Parameters Based on Relative Galaxy Ages*. ApJ, **573**, 37, (2002).
- [69] M. Moresco et al. *Improved constraints on the expansion rate of the Universe up to $z \sim 1.1$ from the spectroscopic evolution of cosmic chronometers*. JCAP, **08**, 006, (2012).
- [70] C. Zhang, H. Zhang, S. Yuan, S. Liu, T.-J. Zhang and Y.-C. Sun. *Four new observational $H(z)$ data from luminous red galaxies in the Sloan Digital Sky Survey data release seven*. Res. Astron. Astrophys., **14**, 1221, (2014).
- [71] J. Simon, L. Verde and R. Jimenez. *Constraints on the redshift dependence of the dark energy potential*. Phys. Rev. D, **71**, 123001, (2005).
- [72] D. Stern, R. Jimenez, L. Verde, M. Kamionkowski and S. A. Stanford. *Cosmic chronometers: constraining the equation of state of dark energy. I: $H(z)$ measurements*. JCAP, **02**, 008, (2010).
- [73] M. Moresco. *Raising the bar: new constraints on the Hubble parameter with cosmic chronometers at $z \sim 2$* . Mon. Not. Roy. Astron. Soc., **450**, L16, (2015).
- [74] M. Moresco et al. *A 6% measurement of the Hubble parameter at $z \sim 0.45$: direct evidence of the epoch of cosmic re-acceleration*. JCAP, **05**, 014, (2016).
- [75] Planck Collaboration et al. *Planck 2018 results. VI. Cosmological parameters*. A&A, **641**, A6, (2020).
- [76] C. E. Rasmussen. *Gaussian processes in machine learning*. Summer school on machine learning, Springer, (2003).
- [77] L. Kazantzidis and L. Perivolaropoulos. *Hints of a local matter underdensity or modified gravity in the low z Pantheon data*. Phys. Rev. D, **102**, 023520, (2020).
- [78] M. Chevallier and D. Polarski. *Accelerating Universes with Scaling Dark Matter*. Int. J. Mod. Phys. D, **10**, 213, (2001).
- [79] E. V. Linder. *Exploring the Expansion History of the Universe*. Phys. Rev. Lett., **90**, 091301, (2003).
- [80] H. K. Jassal, J. S. Bagla and T. Padmanabhan. *WMAP constraints on low redshift evolution of dark energy*. Mon. Not. Roy. Astron. Soc., **356**, L11, (2005).
- [81] D. Foreman-Mackey, D. W. Hogg, D. Lang and J. Goodman. *emcee: The MCMC Hammer*. Publ. Astron. Soc. Pac., **125**, 306, (2013).
- [82] D. Foreman-Mackey. *corner.py: Scatterplot matrices in Python*. J. Open Source Softw., **1**, 24, (2016).
- [83] H.-N. Lin, M.-H. Li and X. Li. *New constraints on the distance duality relation from the local data*. Monthly Notices of the Royal Astronomical Society, **480**, 3117–3122, (2018).
- [84] A. G. Riess, S. Casertano, W. Yuan, J. B. Bowers, L. Macri, J. C. Zinn and D. Scolnic. *Cosmic Distances Calibrated to 1% Precision with Gaia EDR3 Parallaxes and Hubble Space Telescope Photometry of 75 Milky Way Cepheids Confirm Tension with Λ CDM*. ApJ, **908**, L6, (2021).

- [85] X. Wen and K. Liao. *Calibrating the standard candles with strong lensing*. The European Physical Journal C, **80**, (2020).
- [86] LSST Science Collaboration *et al.* *LSST Science Book, Version 2.0*. arXiv e-prints, arXiv:0912.0201, (2009).
- [87] Ž. Ivezić *et al.* *LSST: From Science Drivers to Reference Design and Anticipated Data Products*. ApJ, **873**, 111, (2019).
- [88] H. Zhan and J. A. Tyson. *Cosmology with the Large Synoptic Survey Telescope: an overview*. Rep. Prog. Phys., **81**, 066901, (2018).
- [89] T. Eifler *et al.* *Cosmology with the Roman Space Telescope - multiprobe strategies*. Mon. Not. Roy. Astron. Soc., **507**, 1746, (2021).
- [90] T. E. Oliphant. *A guide to NumPy*, vol. 1, (Trelgol Publishing USA2006).
- [91] J. D. Hunter. *Matplotlib: A 2D graphics environment*. Comput. Sci. Eng., **9**, 90, (2007).